Original Research *Highlight article*

Efficacy of radiation exposure in laryngeal squamous cell carcinoma is mediated by the LAMP3/LAMC2/tenascin-C pathway

Hao Wu[1,*], Juanjuan Li[1,*], Jianqiu Chen[2], Yong Yin[1], Peng Da[1], Qingwen Chen[1], Zhenxin Zhang[1], Jinxing Wang[3], Guohua Wang[3] and Xiaoxia Qiu[1]

[1]Department of Otorhinolaryngology – Head and Neck Surgery, Nantong University Affiliated Hospital, Nantong, Jiangsu 226001, P.R. China; [2]Department of Otolaryngology – Head and Neck Surgery, General Hospital of Jinan Military Region, Jinan, Shandong 250031, P.R. China; [3]Department of Physiology and Hypoxic Biomedicine, Institute of Special Environmental Medicine, Nantong University, Nantong, Jiangsu 226001, P.R. China

*These authors contributed equally to this research.

Corresponding authors: Xiaoxia Qiu. Email: entqxx@163.com; Guohua Wang. Email: wgh036@hotmail.com

Impact statement

It is important to establish effective early diagnostic indicators and reliable treatment strategies for laryngeal squamous cell carcinoma (LSCC). We previously found that expression of LAMP3 was significantly higher in cancerous tissues compared to adjacent normal surgical margin tissues. The present study explored the role of LAMP3 and the related molecular mechanisms in the efficacy of radiation exposure in LSCC. *In vitro* Transwell and Matrigel assays were performed, and a patient-derived xenograft (PDX) model of LSCC *was* established. Associated signaling pathways downstream of LAMP3 were analyzed using RNA sequencing. Signaling pathways regulated by LAMP3 were clearly identified by combining the PDX model with transcriptome analysis. Reduced LAMP3 expression enhanced the efficacy of radiation exposure in LSCC. Thus, by utilizing this molecule as a marker, specific groups of patients may be screened for targeted therapy in the future.

Abstract

The present study explored the role of LAMP3 and related molecular mechanisms in the efficacy of radiation exposure in laryngeal squamous cell carcinoma (LSCC). A lentivirus vector containing the LAMP3 gene was transfected into HEp-2 cells to construct siRNA-LAMP3 and complementation (siLAMP3+LAMP3) groups. Treatment with 4 Gy or 8 Gy radiation was administered to evaluate the role of LAMP3 in radiation therapy. Apoptosis was detected by Annexin V/propidium iodide double staining. Cell migration and invasion were measured *in vitro* using Transwell and Matrigel assays. Downstream genes regulated by LAMP3 were analyzed using RNA sequencing. Furthermore, a patient-derived xenograft (PDX) model of LSCC was established to verify the efficacy of radiation exposure and the associated signaling pathways downstream of LAMP3. The efficacy of radiation showed that cell proliferation was significantly inhibited by siRNA-LAMP3 knockdown. Increased apoptosis was also observed. Notably, the inhibitory effect was attenuated and apoptosis rates were decreased after LAMP3 complementation. *In vitro* cellular assays showed that migration and invasion were significantly suppressed by siRNA-LAMP3 knockdown and increased after LAMP3 complementation. Analysis of the efficacy of radiation exposure in the PDX model showed that LAMP3-specific knockdown inhibited tumor growth and that tumor growth was further reduced by the combined radiotherapy treatment. According to transcriptome analysis, the extracellular matrix-receptor interaction pathway is regulated by LAMP3, and further analysis revealed significant differences in key-associated molecules, including laminin subunit gamma-2 (LAMC2) and tenascin-C (TNC). Validation of the *in vivo* PDX model using qPCR and Western blot analyses supported the abovementioned results. The present findings suggest that reduced LAMP3 expression enhances the efficacy of radiation exposure in LSCC by regulating the LAMP3/LAMC2/TNC signaling pathway.

Keywords: Laryngeal squamous cell carcinoma, patient-derived xenograft model, LAMP3, radiotherapy, LAMC2, tenascin-C

Experimental Biology and Medicine **2019; 244: 1070–1080. DOI: 10.1177/1535370219867643**

Introduction

Laryngeal cancer is the most common malignant tumor of the larynx and has the second highest incidence among malignancies of the respiratory tract. Laryngeal cancer accounts for approximately 14% of head and neck cancers and 2% of all malignancies. Approximately 96% of laryngeal cancers are squamous cell carcinomas.[1] Furthermore, the pathogenesis of laryngeal squamous cell carcinoma (LSCC) is not fully understood.[2] Due to the lack of effective early diagnosis and prognosis methods, local recurrence and distant metastasis remain the main causes of death from LSCC.[3,4] Therefore, it is of great importance to research effective early diagnostic indicators and to establish more reliable treatment strategies for LSCC.

Lysosome-associated membrane proteins (LAMPs) are key membrane proteins involved in lysosome formation and the maintenance of lysosomal stability; these proteins also serve as lysosomal markers. Five members of this protein family have been discovered to date: LAMP1, LAMP2, LAMP3, CD68/Macrosialin/LAMP4, and BAD-LAMP/LAMP.[5] Proteins in the LAMP family have been implicated in the regulation of multiple cellular processes, such as cell growth, adhesion, and metastasis.[6,7] The main function of LAMP1 and LAMP2 is to maintain the stability of the lysosomal membrane. In contrast, LAMP3, which was initially shown to be a molecular marker of mature dendritic cells (CD208, DC-LAMP),[8] is closely associated with tumors. The LAMP3 gene is located on chromosome 3q27, and gene amplification has confirmed that this region is closely related to various tumors.[9,10]

Bisio *et al*. have demonstrated that LAMP3 is upregulated in response to doxorubicin and fluorouracil (5FU) and influences cell migration,[11,12] and Nagelkerke *et al.* showed that LAMP3 is involved in the resistance of breast cancer cells to tamoxifen.[13] Our previous immunohistochemical staining results showed that expression of LAMP3 in LSCC differs significantly from that in corresponding adjacent tissues. Furthermore, the correlation between LAMP3 and antitumor treatments has been experimentally confirmed in recent years, including the finding that hypoxia in LSCC can promote the development of radiotherapy tolerance.[11] Nonetheless, the molecular mechanism underlying the regulatory effect of LAMP3 on these cellular behaviors remains to be elucidated.

To further understand LSCC development, it is particularly important to establish an appropriate animal model to simulate the clinical characteristics of tumors. In patient-derived tumor xenografts (PDXs) from human tissues, the basic characteristics of tumor tissues, including the microenvironment and histopathology, can be well preserved, thereby providing a suitable *in vivo* model for tumor research.[14,15] The expression levels of LAMP3 can be effectively manipulated in mice in a PDX model to determine the efficacy of radiation exposure on tumors. By combining the PDX model with transcriptome analysis, the signaling pathways regulated by LAMP3 can be clearly identified. Thus, by using this molecule as a marker, specific groups of patients may be screened for targeted therapy in the future.

Materials and methods

Materials

The human laryngeal carcinoma cell line HEp-2 was purchased from Procell Life Science & Technology (short tandem repeat (STR) identification provided; Wuhan, China). The tumor sample was obtained from a patient with glottic squamous cell carcinoma. The full-length LAMP3 gene was constructed by General Biosystems (Anhui, China), and fragments for LAMP3 knockdown were designed and synthesized by GenePharma (Suzhou, China). LV5 lentivirus vector packaging was carried out by Obio Technology (Shanghai, China). Transcriptome sequencing was performed by OE Biotech (Shanghai, China). Specific-pathogen-free (SPF) NOD SCID mice and nude mice were provided by the Experimental Animal Center of Nantong University and fed in strict accordance with the standard requirements for SPF animals; food and water were available *ad libitum*. The study protocol was approved by the Human Research Ethics Committee of the Affiliated Hospital of Nantong University, and all study participants provided written informed consent prior to their participation in the study.

Methods

Cell lines and cell culture

HEp-2 cells were cultured in Dulbecco's modified Eagle's medium (DMEM) supplemented with 10% fetal bovine serum (FBS; Gibco, USA), 100 IU/mL penicillin and 100 mg/mL streptomycin (Life Technologies, USA). All cells were cultured in an incubator at 37 °C in an atmosphere containing 5% CO_2.

Cell transfection

siRNA-LAMP3 was designed using online software and synthesized by GenePharma. The siRNA sequences used were as follows (in pairs, sense, and antisense): LAMP3-siRNA1, 5′-CACGAUGGCAGUCAAAUGATT-3′ and 5′-UCAUUUGACUGCCAUCGUGTT-3′; LAMP3-siRNA2, 5′-CAACAACUCACA CACAGCUTT-3′ and 5′-AGCUGUGUGUGAGUUGUUGTT-3′; LAMP3-siRNA3, 5′-CCUCGGAGAUACUUCAACATT-3′ and 5′-UGUUGAAGUAUCUCCGAGGTT-3′. A LAMP3 overexpression plasmid was designed in the present study and verified by sequencing. HEp-2 cells were seeded in complete medium without antibiotics, and transfection was performed when the cells reached 80–90% confluence using Lipofectamine 2000 according to the manufacturer's instructions. For the LAMP3 complementation group, LAMP3 overexpression plasmids were transfected into cells at 48 h after transfection with siRNA-LAMP3.

RNA extraction and quantitative real-time polymerase chain reaction analysis

For qRT-PCR analysis, total RNA was isolated from HEp-2 cells using TRIzol reagent (Invitrogen, Carlsbad, USA) according to the manufacturer's protocol. After the RNA

concentration was measured, 2 μg was subjected to reverse transcription using a cDNA synthesis kit (Tiangen Biotech, China), and the remaining RNA samples were stored at −80°C. Real-time quantitative PCR was then performed with a Corbett Research Rotor-Gene 3000 Real-time Thermal Cycler (Corbett Research, Cambridge, UK) and SYBR Green Detection Kit (Invitrogen). Relative expression levels were assessed using the $2^{-\Delta\Delta CT}$ method. Data analysis was carried out using SPSS 17.0 statistical software, and mapping was conducted using SigmaPlot 10.0 mapping software. The following sequences were used: LAMP3, sense 5′-TGTGCTTCCTGTGATTGGGG-3′ and antisense 5′-CCCCCGGGCAACAATTAGA-3′; *β*-actin, sense 5′-GATGAGATTGGCATGGCTTT-3′ and antisense 5′-GTCACCTTCACCGTTCCAGT-3′.

Protein extraction and Western blot analysis

Total proteins were extracted from cells for 30 min on ice using radioimmunoprecipitation assay (RIPA) lysis buffer (50 mM Tris-HCl, pH 7.4, 150 mM NaCl, 0.2% sodium dodecyl sulfate (SDS), 1% Triton X-100, 2 mM EDTA). The protein concentration was determined using a bicinchoninic acid (BCA) quantification kit (Beyotime, Beijing, China). Protein lysates (50 μg) were separated by 12% SDS-PAGE and blotted onto 0.45-μm polyvinylidene difluoride (PVDF) membranes (Millipore, Hercules, CA). The membranes were blocked with 5% nonfat milk (w/v) at room temperature for 1 h and incubated overnight at 4 °C with anti-laminin subunit gamma-2 (LAMC2) and anti-tenascin-C (TNC) primary antibodies, which were diluted to 1:1000 (Abcam, USA). The membranes were then incubated with horseradish peroxidase conjugated secondary antibody (Jackson, USA) at room temperature for 2 h. Immunoreactivity was visualized using an enhanced chemiluminescence (ECL) Western blotting kit (Invitrogen) according to the manufacturer's protocols. Glyceraldehyde 3-phosphate dehydrogenase (GAPDH) was employed as a loading control. All experiments were performed independently in triplicate.

BrdU cell division assay

siRNA-LAMP3 and LAMP3 complementation groups were irradiated with 4 Gy and 8 Gy (1 Gy indicates that 1 kg of irradiated material absorbed 1 J of energy). The nucleic acid substitute 5-bromo-2-deoxyuridine (BrdU) is incorporated into daughter cells, with BrdU signals, when parent cells symmetrically divide; however, when cells undergo asymmetric division, only one daughter cell exhibits a BrdU signal. Thus, BrdU can be used to observe asymmetric cell division. For observation of asymmetric cell division, the cells were labeled with BrdU at 24 h before irradiation.

RNA sequencing

siRNA-LAMP3 and LAMP3 complementation groups were collected, and total RNA was extracted. The integrity of the RNA was determined by agarose gel electrophoresis. The concentration and purity of the RNA were measured using a spectrophotometer with RNase-free water as a reference. Qualified RNA samples were sent to OE Biotech (Shanghai, China) for transcriptome sequencing, and differential expression of downstream signaling pathways was analyzed.

Flow cytometry analysis of apoptosis

HEp-2 cells were seeded in 6-well plates at a density of 2×10^5 cells per well. When 70–80% confluence was reached, the cells were transfected with LAMP3-silencing and LAMP-overexpression plasmids for 48 h. Cells were collected for processing in accordance with the instructions provided with the apoptosis kit (BD Biosciences, San Jose, USA) using a flow cytometer (Beckman Coulter, Brea, USA). Data were processed and analyzed using a Beckman Coulter Epics XL flow cytometer.

Cell viability

HEp-2 cells were seeded in a 96-well plate at a density of 6000 cells per well in 100 μL of medium. Lipofectamine 2000 reagent was used for transfection of LAMP3-silencing and LAMP-overexpression plasmids, and cell viability was assessed using an MTT assay at 48 h after transfection. Each well was supplemented with 10 μL of 5 mg/mL MTT (Sigma-Aldrich, St. Louis, USA) and incubated for 4 h; the MTT solution was removed, and dimethyl sulfoxide was added to each well to dissolve the metabolic product. Absorbance at 490 nm was measured using a microplate reader (Thermo Fisher Scientific Inc.).

Transwell chamber-matrigel invasion and migration assays

Matrigel-coated 24-well Transwell plates (8 μm pore size; BD Biosciences) were used for the cell invasion assay. The same number (1×10^5) of cells transfected with the LAMP3-silencing or LAMP3-overexpression plasmids or untransfected was resuspended in serum-free medium and added to the upper chamber. In the lower chamber, 2% FBS in DMEM was added as a chemoattractant. After 24 h of incubation, noninvading cells on the upper wells were removed with a cotton-tipped swab; cells on the lower side of the filters were fixed in 4% paraformaldehyde for 10 min and stained with 0.1% crystal violet for 30 min. Images were captured, and the cell count in at least five random microscopic fields was calculated (magnification, ×200). For the migration assay, transfected cells were plated and cultured until 80–90% confluence. An AP-20 micropipette tip was then used to generate a scratch in the monolayer. Migration ability was determined by comparing the widths of the scratches, which were measured at 0 h and 24 h using a bright field microscope.

Establishment of a PDX model of LSCC

NOD/SCID mice (four to six weeks old) were fed in an SPF barrier environment and allowed to acclimatize for more than three days before the experiment. Surgery was performed to obtain tumor tissues from patients, and the samples were stored in ice-cold RPMI-1640 medium (supplemented with 20% FBS and 0.05% penicillin/streptomycin) and

transplanted into the mice as soon as possible. To this end, tumor tissue necrosis sites and broken tissue were removed, and the tumor tissue was diced into cubes approximately $2 \times 2 \times 3$ mm^3 in size. After the mice were anesthetized, the diced tumor tissue was transplanted into the subcutaneous space and the kidney capsule, and the incision was sutured. The remaining tissues were preserved in liquid nitrogen or embedded in paraffin. The xenograft was subcultured when it grew to 1000–1500 mm^3. Briefly, the tumor-bearing mice were sacrificed by cervical dislocation and the mice were soaked in 75% alcohol for 2 min, and the tumor tissue was removed. The tumor tissue was inoculated as described above. The tumor at the third passage was subject to drug testing after growing to 100–200 mm^3. In general, tumors at the third to seventh passage were used in experiments.

Effect of LAMP3 silencing on radiation susceptibility

The PDX model of LSCC at the third to seventh passage was used for efficacy evaluation. When the transplanted tumor grew to 100–200 mm^3, the animals were randomly divided into groups ($n = 3$ in each group) and were accordingly treated as follows: (1) negative control siRNA lentivirus (50 mg/kg/3 day); (2) X-ray irradiation at 8 Gy; (3) siRNA-LAMP3 lentivirus (50 mg/kg/3 day) by intraperitoneal injection; or (4) siRNA-LAMP3 lentivirus (50 mg/kg/3 day) + radiotherapy for two weeks. The appetite, movement, and mental state of the mice, in addition to any side effects of LAMP3 silencing and the size of the tumors, were observed with every treatment administration. After two weeks of treatment, the relative tumor inhibition rates of each treated group vs. the control group were evaluated. The relative tumor growth inhibition (TGI) was calculated as TGI $=1-T/C$, where T/C represents the tumor volume of the treated group/tumor volume of the control group. The tumor volume of was measured every 3 days and calculated as (long diameter $\times$ short diameter^2)/2.

Statistical analysis

Differences between groups were determined by one-way ANOVA using SPSS v17.0 (IBM Co.). All experiments were repeated at least three times. All data are expressed as the mean $\pm$ standard deviation. $P < 0.05$ was considered statistically significant.

Results

Validation of LAMP3 silencing efficiency

HEp-2 cells were collected 48 h after LAMP3 knock-down, and RNAs were extracted. The expression levels of LAMP3 were detected by qRT-PCR and Western blot analysis (Figure 1(a) and (b)). Efficient targeting of LAMP3 by siRNAs was achieved, and we selected LAMP3-siRNA1, which was the most effective at reducing LAMP3 levels, for further studies.

HEp-2 cells were cultured in 6-well plates and transfected with LAMP3-siRNA1 using Lipofectamine 2000; the LAMP3-overexpressing plasmid was transfected into the cells 48 h later, and the LAMP3 complementation rate was detected after an additional 48 h. The results suggested that the expression level of LAMP3 after complementation was higher than that in the LAMP3-siRNA group (Figure 1(c) and (d) ($^{**}P < 0.01$ vs. the control; $^{\#\#}P < 0.01$ vs. the LAMP3-siRNA group).

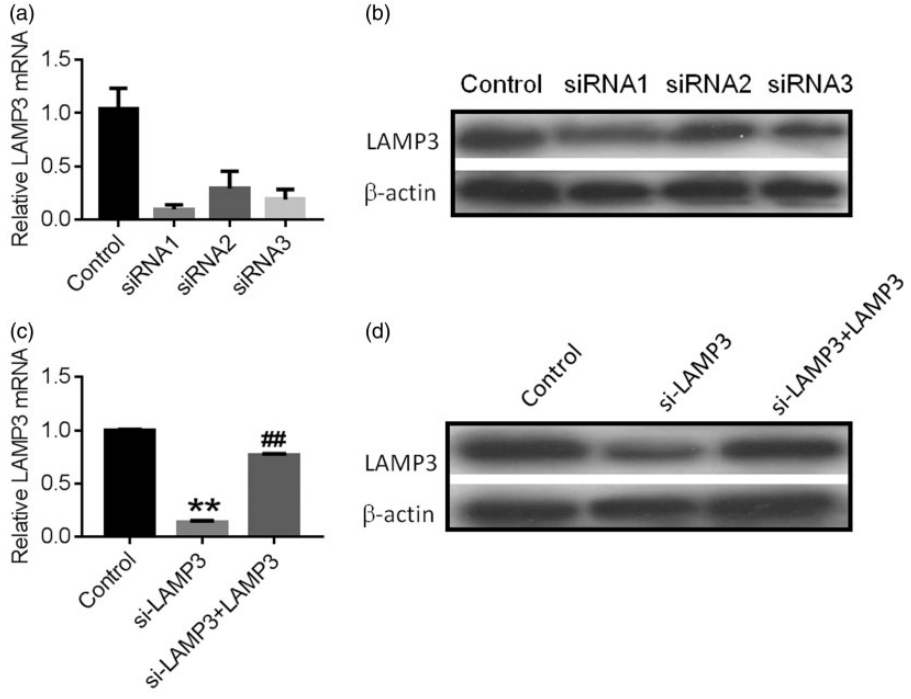

Figure 1. The expression level of LAMP3 was detected by qRT-PCR and Western blot analysis. (a and b) As shown, the optimal knockdown effect was noted with LAMP3-siRNA1, which was used in the subsequent experiments. (c and d) The expression level of LAMP3 after complementation was higher than that in the siRNA-LAMP3 group. $^{**}P < 0.01$ vs. the control; $^{\#\#}P < 0.01$ vs. the siRNA-LAMP3 group.

Effect of LAMP3 expression on cell proliferation ability

HEp-2 cells were cultured in 96-well plates and transfected with LAMP3-silencing and LAMP3-overexpression plasmids using Lipofectamine 2000. Cell proliferation was determined by an MTT assay at 48 h after transfection, with three replicates for each group. According to the results, cell proliferation was significantly inhibited and apoptosis increased after LAMP3 knockdown. Furthermore, the inhibitory effect was attenuated and apoptosis decreased after LAMP3 complementation (Figure 2) (**$P < 0.01$, vs. the control; $^{\#\#}P < 0.01$ vs. the siRNA-LAMP3 group).

Effect of LAMP3 expression on cell migration and invasion abilities

HEp-2 cells were cultured in 60-mm dishes and transfected with siRNA-LAMP3 or the LAMP3-overexpression plasmid using Lipofectamine 2000, and Transwell assays were used to detect the migration and invasion abilities of the cells. The results showed that the migration and invasion abilities of the cells were significantly inhibited by siRNA-LAMP3 but that LAMP3 complementation reversed this inhibition induced by siRNA-LAMP3 (Figure 3) (**$P < 0.01$ vs. the control; $^{\#\#}P < 0.01$ vs. the siRNA-LAMP3 group).

Assessment of asymmetric cell division by the BrdU assay

HEp-2 cells were irradiated with different doses of radiation after LAMP3 knockdown or complementation, and proliferation was detected using a BrdU assay. Targeting LAMP3 with siRNA significantly inhibited cell proliferation, and LAMP3 complementation reversed this inhibition (Figure 4).

Efficacy of radiation exposure in the PDX mouse model *in vivo*

As shown in Figure 5(a) and (b), tumor volumes were significantly reduced at 12 days after treatment in the groups that received radiotherapy or LAMP3 silencing alone compared with the control group ($P < 0.05$). In addition, tumor sizes in the group that received radiotherapy and LAMP3

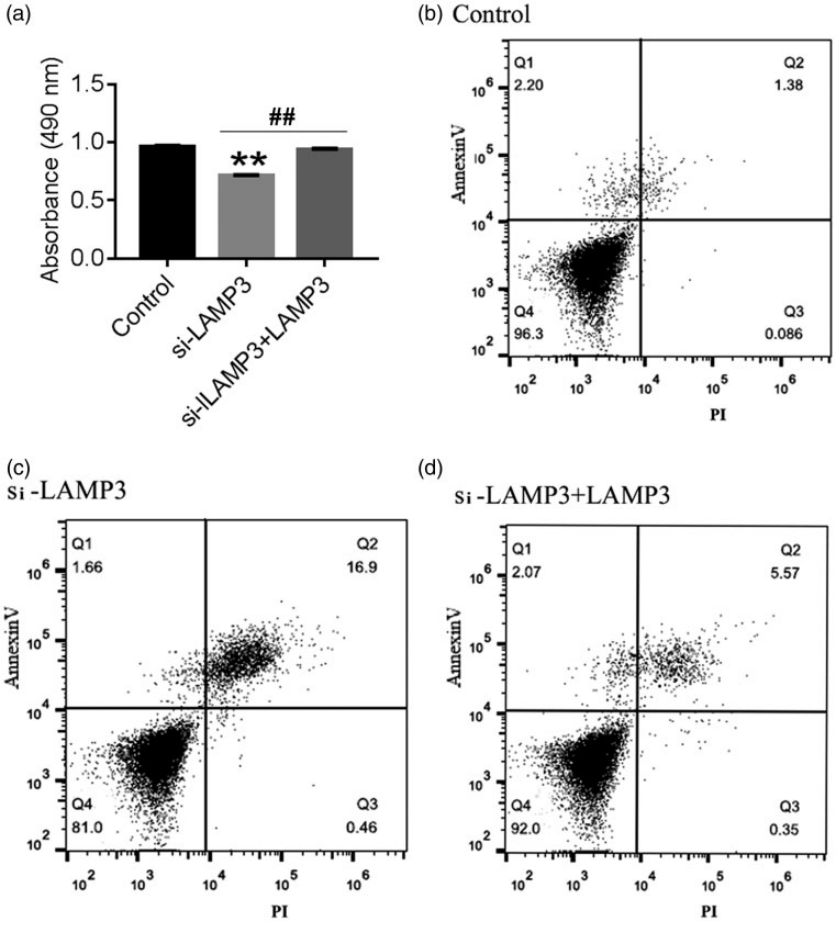

Figure 2. The effect of LAMP3 on cell viability and apoptosis in HEp-2 cells. (a) Measurements of cell viability from cultured HEp-2 cells after LAMP3 knockdown or overexpression. HEp-2 cells were cultured in 96-well plates. LAMP3 knockdown and overexpression plasmids were transfected into cells using Lipofectamine 2000. After 48 h, the proliferation of HEp-2 cells was measured by the MTT assay. (b, c and d) Apoptosis in HEp-2 cells was assessed using the Annexin V-FITC/PI Apoptosis Detection kit, and fluorescence-activated cell sorting analysis was performed. The upper right quadrant (Q2; Annexin V^+/PI^+) indicates apoptosis. Cell proliferation was significantly inhibited and apoptosis increased after LAMP3 knockdown; however, the inhibitory effect was attenuated and apoptosis decreased after LAMP3 complementation. The experiment was performed in triplicate, and representative data are shown. **$P < 0.01$ vs. the control; $^{\#\#}P < 0.01$ vs. the siRNA-LAMP3 group.

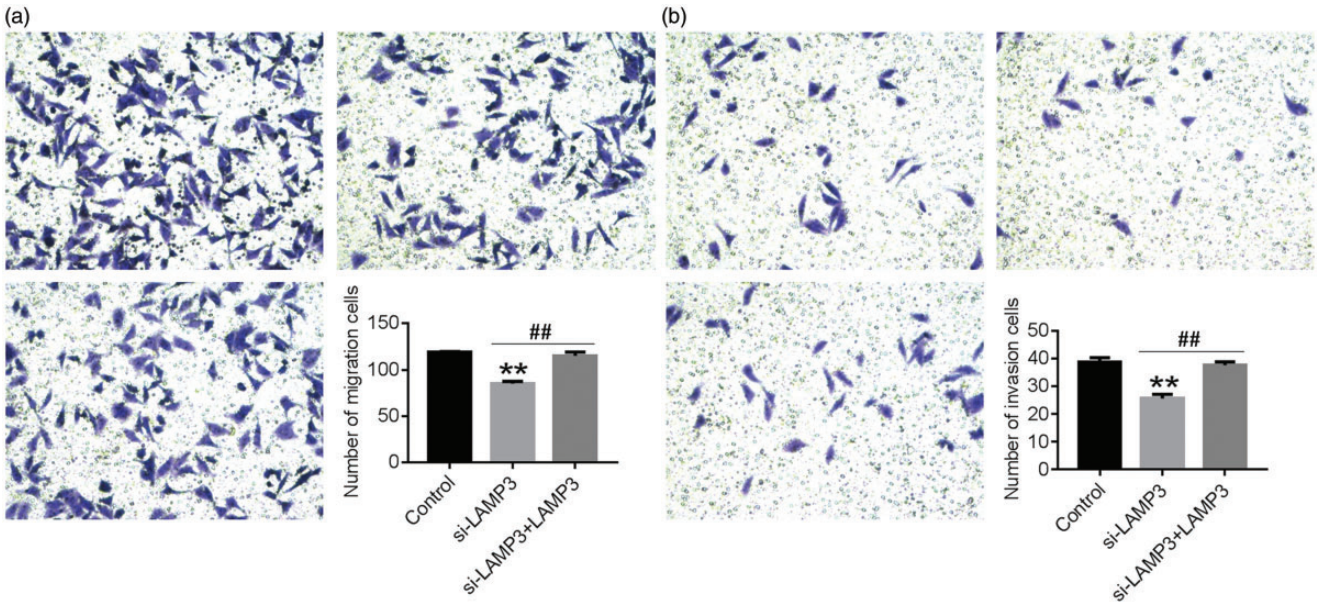

Figure 3. The effect of LAMP3 on the migration and invasion of HEp-2 cells. (a) The results suggested that the migration abilities of the cells were significantly inhibited by siRNA-LAMP3 and increased after LAMP3 complementation. (b) The results also suggested that the invasion abilities of the cells were significantly inhibited by siRNA-LAMP3 and increased after LAMP3 complementation. $^{**}P < 0.01$ vs. the control; $^{\#\#}P < 0.01$ vs. the siRNA-LAMP3 group. (A color version of this figure is available in the online journal.)

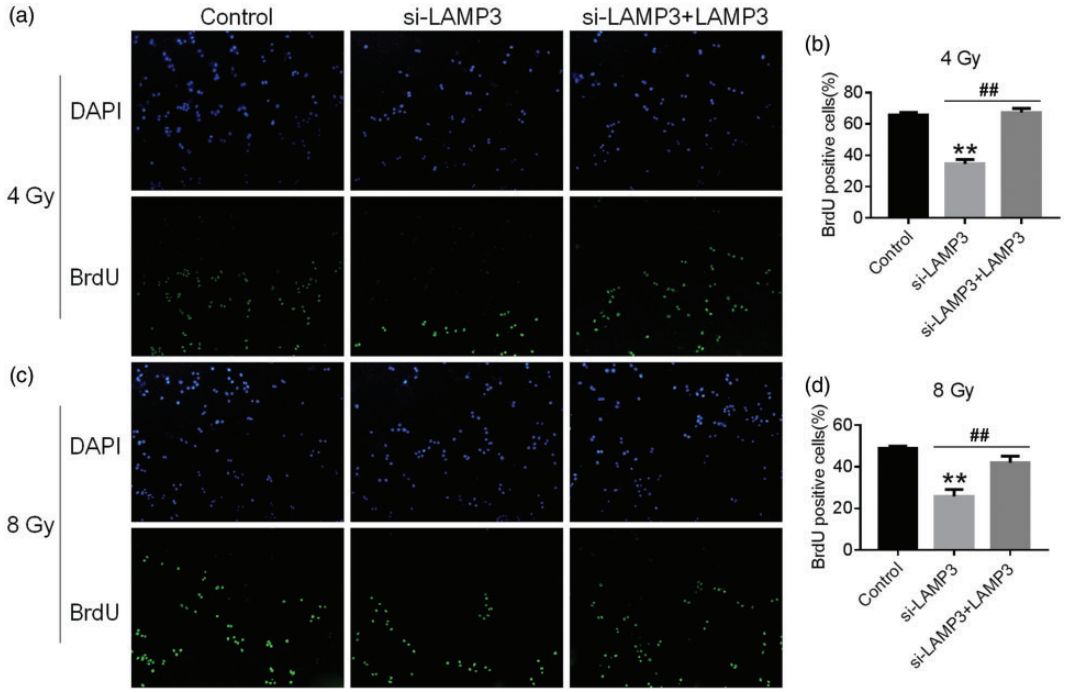

Figure 4. The effect of LAMP3 on the proliferation of HEp-2 cells after treatment with 4 Gy and 8 Gy of radiation. HEp-2 cells were irradiated with 4 Gy of radiation (a) or 8 Gy of radiation (b) after LAMP3 silencing and complementation. (c) Cell proliferation was assessed using the BrdU assay, and the results are presented as the ratio of the number of BrdU-positive cells to the number of DAPI-positive cells. $^{**}P < 0.01$ vs. the control; $^{\#\#}P < 0.01$ vs. the siRNA-LAMP3 group. (A color version of this figure is available in the online journal.)

silencing were significantly different from those in the control group at 6 days after treatment (Figure 5(b), $P < 0.05$), and this significant difference was greater on days 9 and 12 (Figure 5(b), $P < 0.01$). Compared with the group that received radiotherapy alone or LAMP3 knockdown alone, the tumor volume of the combined treatment group was significantly reduced (Figure 5(b), $P < 0.05$).

Transcriptome sequencing analysis

According to RNA-seq, the expression profile of the siRNA-LAMP3 group was significantly different from that of the control and LAMP3 complementation groups. Changes in the expression levels of the same gene in each sample were analyzed using $P < 0.05$ and a difference multiple of

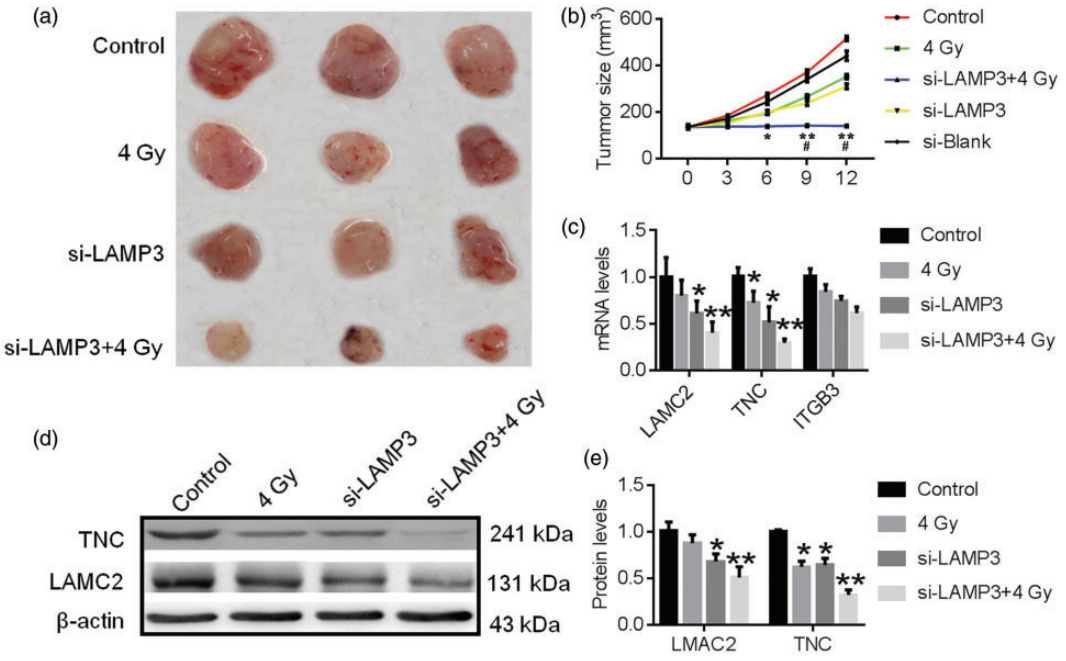

Figure 5. Tumor sizes of patient-derived xenograft (PDX) model mice in the different treatment groups and differential gene expression verified by qPCR and Western blot analyses. (a) Representative images of tumors excised three generations after implantation and 12 days after irradiation. (b) The tumor volume curve of the different treatment groups at different time points. The radiation dose that each animal received in this experiment was 4 Gy. "Day 0" is the day of irradiation. Gy is an SI unit of absorbed radiation. $^{*}P < 0.05$, $^{**}P < 0.01$ vs. the control group; $^{\#}P < 0.05$ vs. the Gy or siRNA-LAMP3 group. (b) (c, d and e) qPCR and Western blot analysis verification in the different groups of PDX mice demonstrated that the gene and protein expression levels of LAMC2 and tenascin-C in the siRNA-LAMP3 group were significantly downregulated, which supported the results from RNA-seq. Expression of ITGB3, a gene in the ECM-receptor pathway, was not significantly altered in the PDX model mice subjected to different treatments. $^{*}P < 0.05$, $^{**}P < 0.01$ vs. the control group. (A color version of this figure is available in the online journal.)

>2 as the default screening criteria. The results showed that 358 genes were upregulated and 258 genes downregulated in the siRNA-LAMP3 group compared to the control group (Figure S1A). Furthermore, 260 genes were upregulated and 340 genes downregulated in the siRNA-LAMP3 group compared to the LAMP3 complementation group (Figure S1B). Gene ontology (GO) enrichment analysis of the differentially expressed genes was conducted to examine functions, and 30 categories of genes were identified, with the most significant differences between the siRNA-LAMP3 group and the control group as well as the complementation group (Figure 6). Furthermore, comprehensive comparison revealed that the most significant difference was linked to functions related to the regulation of apoptosis and angiogenesis. Pathway analysis of differential genes was also performed using the Kyoto Encyclopedia of Genes and Genomes (KEGG) database, and the significance of the differential enrichment of each pathway item was calculated using a hypergeometric distribution test. A total of 20 pathways were identified, and the most significant difference was observed between the siRNA-LAMP3 group and the control group as well as the complementation group (Figures S2 and S3). Comprehensive comparison showed that the pathways most regulated by LAMP3 included the estrogen signaling pathway and the extracellular matrix (ECM) receptor interaction pathway. Thus, LAMP3 is mainly involved in the cellular response in LSCC, a pathway that is responsible for amplifying external signals.

Further analysis revealed that the key molecules in the ECM-receptor interaction pathway, LAMC2 and TNC, were differentially expressed. Based on qPCR and Western blot analyses performed using the different PDX model groups, the gene and protein expression levels of LAMC2 and TNC in the siRNA-LAMP3 group were significantly downregulated, which also supported the RNA-seq results ($P < 0.05$; Figure 5(c) to (e)). Notably, the reduction in tumor volume after treatment was more significant when the expression levels of LAMC2 and TNC were lower (Figure 5(d) and (e)). However, expression of ITGB3, a gene in the ECM-receptor pathway, in the PDX model was not significantly altered following different treatments ($P > 0.05$; Figure 5(c)).

Discussion

It has been reported that the incidence of LSCC is closely related to lifestyle factors, including smoking and alcohol consumption.[2] Because of growing aging population, high smoking rate and environmental pollution, the morbidity and mortality of laryngeal cancer in China remain a cause for concern. Overall, the development of LSCC is a complex process involving multiple factors and stages. Early-stage LSCC patients are usually treated with radiotherapy or laryngeal preservation surgery, whereas advanced-stage patients need to be individually treated after balancing the total survival time with quality of life. Due to the lack of effective early diagnosis methods and poor prognosis, local recurrence and distant metastasis are the primary causes of death from LSCC.[3,4] In the present research, the

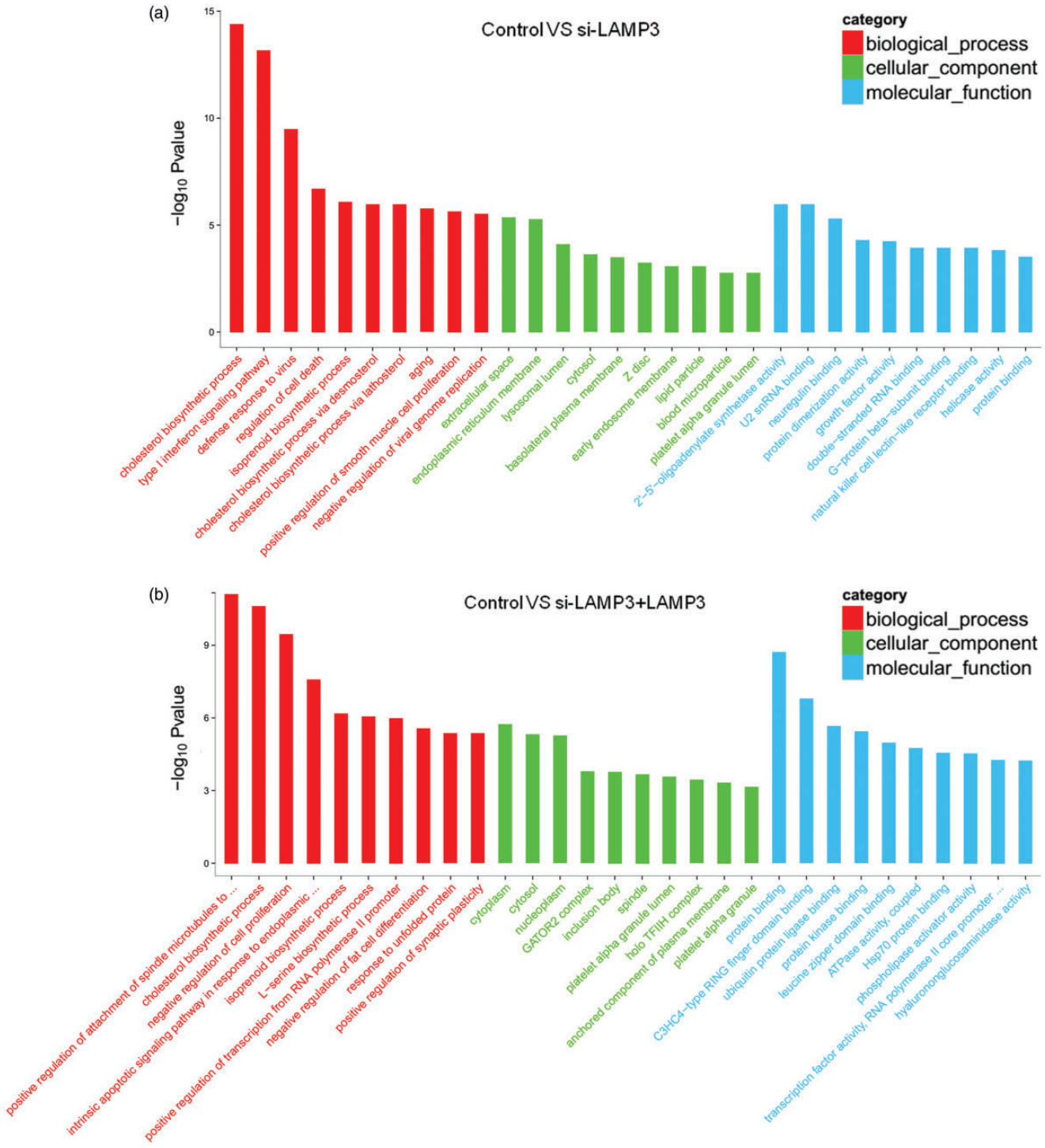

Figure 6. Transcriptome analysis results. Pathway analysis of differentially expressed genes was performed using the KEGG database. The significance of differentially expressed gene enrichment in each pathway was calculated using the hypergeometric distribution test. A total of 20 pathways were identified, and the most significant difference was observed between the siRNA-LAMP3 group (a) and the control group as well as the complementation group (b). (A color version of this figure is available in the online journal.)

main goal was to explore the effect of LAMP3 on the efficacy of radiation exposure in LSCC and the related molecular mechanisms in an effort to provide guidance for individualized treatment of LSCC patients.

To further explore the molecular mechanism of LAMP3 regulation and its role in tumor development, we constructed specific LAMP3-silencing and -postsilencing complementation systems using HEp-2 cells. siRNA-LAMP3 exhibited significant knockdown efficiency at both the cellular level *in vitro* and *in vivo* in LSCC PDX mice; the knockdown effect of siRNA-LAMP3 was reversed by LAMP3 complementation. To determine the efficacy of exposure to radiation, the overexpression and knockdown systems as well as LSCC PDX nude mice were treated with

irradiation, resulting in significant changes. For the *in vitro* experiments, three different LAMP3-siRNAs were constructed for transfecting HEp-2 cells. qRT-PCR and Western blot analyses showed that the gene and protein expression levels of LAMP3 were most significantly reduced by siRNA1, with the highest knockdown efficiency. Therefore, siRNA1 was used in subsequent experiments. The LAMP3-overexpressing plasmid was used for complementation after knockdown, and the level of LAMP3 expression in the complementation group was significantly higher than that in the siRNA-LAMP3 group. The effects of LAMP3 on the development of tumors were analyzed using the specific LAMP3-silencing and -postsilencing complementation systems. Cell proliferation was detected by the MTT assay and apoptosis by Annexin V/PI double staining in the LAMP3-inhibited, LAMP3-complementation, and control treatment samples. Cell proliferation was significantly suppressed and apoptosis significantly increased after LAMP3 knockdown; however, this inhibition of cell proliferation was attenuated and apoptosis reduced after LAMP3 complementation. Similarly, cell invasion and migration were significantly suppressed after LAMP3 knockdown but were increased after LAMP3 complementation.

It has been reported that LAMP3 can induce migration and invasion in tumor cells *in vitro* and that LAMP3 is strongly involved in tumor metastasis and resistance to treatment.[16,17] Our *in vitro* experiments support these findings. In the present study, cells with LAMP3 silencing and complementation were treated with 4 Gy and 8 Gy X-ray irradiation. Notably, cell proliferation analysis using the BrdU assay demonstrated that cell proliferation in the siRNA-LAMP3 group at both doses was significantly inhibited and that the proliferation ability was significantly increased after LAMP3 complementation, consistent with the findings of Pennati *et al.*[18] and Nagelkerke *et al.*[18,19] Therefore, based on the above results, we speculate that it may be feasible to use LAMP3 as a marker for the treatment of LSCC. In addition to the fact that the PDX model can objectively reflect primary tumors, tumor tissue can be transplanted into several mice while maintaining the highly consistent physicochemical characteristics of the tumor, and multiple tumor models that exhibit the same tumor clinical features can be established for real-time monitoring of the occurrence, development, and treatment of tumors.[20] A large number of human tumor tissue-derived PDX models have been established recently, including for breast cancer, colorectal cancer, and non-small cell lung cancer models.[20–23] In the present study, an LSCC PDX model was treated with radiotherapy alone, LAMP3 knock-down alone, or both together at different time points. The results showed a significant reduction in tumor volume in the single treatment groups at 12 days posttreatment compared with that in the control group. Furthermore, a significant reduction in tumor size was observed in the combined treatment group at six days posttreatment compared that in the control group, and the tumor size was further decreased in the combined treatment group on days 9 and 12. Additionally, tumor sizes in the combined treatment group were significantly reduced compared to those in the radiotherapy-only and LAMP3 silencing-only groups. The above *in vivo* results were consistent with the findings from *in vitro* cell experiments, indicating that the combined application of radiotherapy and LAMP3 silencing is superior to each treatment alone, which further illustrates the profound significance of LAMP3 in the treatment of LSCC.

To explore the signaling pathways that are mediated by LAMP3, transcriptome sequencing was performed in the present study. Pathways clearly regulated by LAMP3 during the occurrence and development of LSCC included the estrogen signaling pathway and the ECM-receptor interaction pathway. Laryngeal cancer was identified as the second most common respiratory system malignancy with LSCC being the most common malignant tumor of the larynx.[24] Larynx being a secondary sex organ showing physiological changes during puberty, raises inquiry about the relationship between sex hormones receptors as estrogen receptors (ER), progesterone receptors (PR), androgen receptors (AR) and the development of laryngeal carcinoma.[24] According to our transcriptome analysis, the estrogen signaling pathway was clearly regulated by LAMP3 during the occurrence and development of LSCC. In recent years, the expression and function of AR and ER in LSCC have been increasingly emphasized.[25] Consistency with our findings, these studies indicate that the sex-related hormone receptors play an important role in the development of LSCC. ER-α and ER-β may be considered as markers for poor biological behavior of laryngeal carcinoma.

In this study, the extracellular matrix-receptor interaction pathway is also regulated by LAMP3, and further analysis revealed significant differences in key associated molecules, including LAMC2and tenascin-C TNC by the transcriptome analysis. And, qPCR and Western blot results verified that the gene and protein expression levels of LAMC2 and TNC were both significantly downregulated in the LAMP3-siRNA group, which was consistent with the transcriptome sequencing results. The protein encoded by the LAMC2 gene in humans is a member of the ECM glycoprotein family, is the major noncollagen component of the basement membrane and involved in the development and progression of a variety of tumour types.[26] Including oral squamous cell carcinoma (OSCC), lung esophageal adenocarcinoma, and non-small cell lung cancer, the overexpression of LAMC2 was also associated with poor clinical outcome. Furthermore, LAMC2 was positively correlated with lymph node metastasis and negatively correlated with the survival rate of colorectal cancer patients.[27]

TNC plays an important role in cancer cell proliferation and migration and tumor invasion in various types of cancer. TNC can directly or indirectly affect the invasiveness and metastatic potential of carcinoma tumors. TNC expression has also been correlated with lymph node metastasis in breast, colon, liver, and oral squamous cell carcinoma.[28] In addition, high expression of TNC could be a useful marker in cancer-associated fibroblasts for determining prognosis in esophageal squamous cell carcinoma (ESCC).[29]

As mentioned above, LAMC2 and TNC seem to contribute to predict poor prognosis in OSCC or ESCC. Similarly,

here we found tumor volumes of LSCC decreased after the corresponding treatment when the expression levels of LAMC2 and TNC were reduced, indicating that the changes in LSCC mediated by LAMP3 may be associated with the effects of LAMC2 and TNC expression. It is possible that the expression of these two molecules of ECM seemed to be biologically meaningful within the process of squamous cell carcinoma progression. However, the identity of the cellular signals that LAMP3 regulate LAMC2 and TNC levels in LSCC is not yet clear. In addition, expression of ITGB3, a gene related to the ECM-receptor pathway, was not significantly altered in tumor tissues from the differently treated PDX model mice. Future studies may wish to apply the coimmunoprecipitation (co-IP) to distinguish the direct or indirect effects of LMAP3 to control LMAC2 and TNC.

In conclusion, the findings of experiments using the constructed LSCC PDX model and cells in the present study suggest that reduced LAMP3 expression enhances the efficacy of radiation exposure in LSCC, which may be a result of regulation of the LAMC2/TNC signaling pathway. The findings provide guidance for individualized treatment of patients with LSCC.

Authors' contributions: WH, LJJ and YY performed the experiments and data collection. WH, CJQ, DP and CQW analyzed and interpreted the data. LJJ, CJQ, WJX and YY wrote and reviewed the manuscript. WH and QXX conceived and supervised the entire project. WGH and QXX revised the manuscript and provided supporting material. All authors read and approved the final manuscript.

DECLARATION OF CONFLICTING INTERESTS

The author(s) declared no potential conflicts of interest with respect to the research, authorship, and/or publication of this article.

FUNDING

This study was supported by Grants from the Funding for Jiangsu 'Six Talent Peaks' foundation (QXX, 2014-WSW-030) and Nantong Science and Technology Project (NS12017012-1, MS12018029).

ETHICS APPROVAL AND CONSENT TO PARTICIPATE

All procedures involving human participants were performed in accordance with the ethical standards of the Nantong University Affiliated Hospital and with the 1964 Declaration of Helsinki and its later amendments or comparable ethical standards. Informed consent was obtained from all participants included in the study.

AVAILABILITY OF DATA AND MATERIALS

All original data are available upon request.

ORCID iD

Guohua Wang https://orcid.org/0000-0002-4810-8534

REFERENCES

1. Dundar R, Aslan H, Ozbay C, Basoglu S, Guvenc IA, Ogredik EA, Ozturkcan S, Tayfun MA, Katilmis H. The necessity of dissection of level IIb in laryngeal squamous cell carcinoma: a clinical study. *Otolaryngol Head Neck Surg* 2012;**146**:390–4
2. Maurya SS, Katiyar T, Dhawan A, Singh S, Jain SK, Pant MC, Parmar D. Gene-environment interactions in determining differences in genetic susceptibility to cancer in subsites of the head and neck. *Environ Mol Mutagen* 2015;**56**:313–21
3. Qiu X, You Y, Huang J, Wang X, Zhu H, Wang Z. LAMP3 and TP53 overexpression predicts poor outcome in laryngeal squamous cell carcinoma. *Int J Clin Exp Pathol* 2015;**8**:5519–27
4. Rodrigo JP, Martinez P, Allonca E, Alonso-Duran L, Suarez C, Astudillo A, Garcia-Pedrero JM. Immunohistochemical markers of distant metastasis in laryngeal and hypopharyngeal squamous cell carcinomas. *Clin Exp Metastasis* 2014;**31**:317–25
5. Alessandrini F, Pezze L, Ciribilli Y. LAMPs: shedding light on cancer biology. *Sem Oncol* 2017;**44**:239–53
6. Kroemer G, Jaattela M. Lysosomes and autophagy in cell death control. *Nat Rev Cancer* 2005;**5**:886–97
7. Saftig P, Klumperman J. Lysosome biogenesis and lysosomal membrane proteins: trafficking meets function. *Nat Rev Mol Cell Biol* 2009;**10**:623–35
8. de Saint-Vis B, Vincent J, Vandenabeele S, Vanbervliet B, Pin JJ, Ait-Yahia S, Patel S, Mattei MG, Banchereau J, Zurawski S, Davoust J, Caux C, Lebecque S. A novel lysosome-associated membrane glycoprotein, DC-LAMP, induced upon DC maturation, is transiently expressed in MHC class II compartment. *Immunity* 1998;**9**:325–36
9. Racz A, Brass N, Heckel D, Pahl S, Remberger K, Meese E. Expression analysis of genes at 3q26-q27 involved in frequent amplification in squamous cell lung carcinoma. *Eur J Cancer* 1999;**35**:641–6
10. Bockmuhl U, Schwendel A, Dietel M, Petersen I. Distinct patterns of chromosomal alterations in high- and low-grade head and neck squamous cell carcinomas. *Cancer Res* 1996;**56**:5325–9
11. Wang M, Li X, Qu Y, Xu O, Sun Q. Hypoxia promotes radioresistance of CD133-positive Hep-2 human laryngeal squamous carcinoma cells in vitro. *Int J Oncol* 2013;**43**:131–40
12. Bisio A, Zamborszky J, Zaccara S, Lion M, Tebaldi T, Sharma V, Raimondi I, Alessandrini F, Ciribilli Y, Inga A. Cooperative interactions between p53 and NFkappaB enhance cell plasticity. *Oncotarget* 2014;**5**:12111–25
13. Nagelkerke A, Sieuwerts AM, Bussink J, Sweep FC, Look MP, Foekens JA, Martens JW, Span PN. LAMP3 is involved in tamoxifen resistance in breast cancer cells through the modulation of autophagy. *Endocrine Relat Cancer* 2014;**21**:101–12
14. Suarez CD, Littlepage LE. Patient-derived tumor xenograft models of breast cancer. *Methods Mol Biol* 2016;**1406**:211–23
15. Whittle JR, Lewis MT, Lindeman GJ, Visvader JE. Patient-derived xenograft models of breast cancer and their predictive power. *Breast Cancer Res* 2015;**17**:17
16. Ozaki K, Nagata M, Suzuki M, Fujiwara T, Ueda K, Miyoshi Y, Takahashi E, Nakamura Y. Isolation and characterization of a novel human lung-specific gene homologous to lysosomal membrane glycoproteins 1 and 2: significantly increased expression in cancers of various tissues. *Cancer Res* 1998;**58**:3499–503
17. Sun R, Wang X, Zhu H, Mei H, Wang W, Zhang S, Huang J. Prognostic value of LAMP3 and TP53 overexpression in benign and malignant gastrointestinal tissues. *Oncotarget* 2014;**5**:12398–409
18. Pennati M, Lopergolo A, Profumo V, De Cesare M, Sbarra S, Valdagni R, Zaffaroni N, Gandellini P, Folini M. miR-205 impairs the autophagic flux and enhances cisplatin cytotoxicity in castration-resistant prostate cancer cells. *Biochem Pharmacol* 2014;**87**:579–97
19. Nagelkerke A, Bussink J, van der Kogel AJ, Sweep FC, Span PN. The PERK/ATF4/LAMP3-arm of the unfolded protein response affects radioresistance by interfering with the DNA damage response. *Radiother Oncol* 2013;**108**:415–21
20. Siolas D, Hannon GJ. Patient-derived tumor xenografts: transforming clinical samples into mouse models. *Cancer Res* 2013;**73**:5315–9

21. Dong X, Guan J, English JC, Flint J, Yee J, Evans K, Murray N, Macaulay C, Ng RT, Gout PW, Lam WL, Laskin J, Ling V, Lam S, Wang Y. Patient-derived first generation xenografts of non-small cell lung cancers: promising tools for predicting drug responses for personalized chemotherapy. *Clin Cancer Res* 2010;**16**:1442–51
22. Julien S, Merino-Trigo A, Lacroix L, Pocard M, Goere D, Mariani P. Characterization of a large panel of patient-derived tumor xenografts representing the clinical heterogeneity of human colorectal cancer. *Clin Cancer Res* 2012;**18**:5314–28
23. Harvey KF, Zhang X, Thomas DM. The Hippo pathway and human cancer. *Nat Rev Cancer* 2013;**13**:246–57
24. Atef A, El-Rashidy MA, Elzayat S, Kabel AM. The prognostic value of sex hormone receptors expression in laryngeal carcinoma. *Tissue Cell* 2019;**57**:84–9
25. Fei M, Zhang J, Zhou J, Xu Y, Wang J. Sex-related hormone receptor in laryngeal squamous cell carcinoma: correlation with androgen estrogen-a and prolactin receptor expression and influence of prognosis. *Acta Otolaryngol* 2018;**138**:66–72
26. Korbakis D, Dimitromanolakis A, Prassas I, Davis GJ, Barber E, Reckamp KL, Blasutig I, Diamandis EP. Serum LAMC2 enhances the prognostic value of a multi-parametric panel in non-small cell lung cancer. *Br J Cancer* 2015;**113**:484–91
27. Zou B, Li J, Xu K, Liu JL, Yuan DY, Meng Z, Zhang B. Identification of key candidate genes and pathways in oral squamous cell carcinoma by integrated Bioinformatics analysis. *Exp Ther Med* 2019;**17**:4089–99
28. Ni WD, Yang ZT, Cui CA, Cui Y, Fang LY, Xuan YH. Tenascin-C is a potential cancer-associated fibroblasts marker and predicts poor prognosis in prostate cancer. *Biochem Biophys Res Commun* 2017;**486**:607–12
29. Yang ZT, Yeo SY, Yin YX, Lin ZH, Lee HM, Xuan YH, Cui Y, Kim SH. Tenascin-C, a prognostic determinant of esophageal squamous cell carcinoma. *PLoS One* 2016;**11**:e0145807

(Received March 3, 2019, Accepted July 12, 2019)